Quaternary Research 80 (2013) 459–467

Contents lists available at ScienceDirect

Quaternary Research

journal homepage: www.elsevier.com/locate/yqres

The deglaciation and neoglaciation of Upernavik Isstrøm, Greenland

Jason P. Briner [a,*], Lena Håkansson [b,c,1], Ole Bennike [b]

[a] Department of Geology, University at Buffalo, Buffalo, NY 14260, USA
[b] Geological Survey of Denmark and Greenland, Øster Voldgade 10, 1350 Copenhagen-K, Denmark
[c] Department of Geology and Mineral Resources Engineering, Norwegian University of Science and Technology, Sem Særlands veg 1, N-7491 Trondheim, Norway

ARTICLE INFO

Article history:
Received 11 July 2013
Available online 21 October 2013

Keywords:
Greenland Ice Sheet
Upernavik Isstrøm
Holocene
Be dating
Lake sediments
Little Ice Age

ABSTRACT

We constrain the history of the Greenland Ice Sheet margin during the Holocene at Upernavik Isstrøm, a major ice stream in northwestern Greenland. Radiocarbon-dated sediment sequences from proglacial-threshold lakes adjacent to the present ice margin constrain deglaciation of the sites to older than 9.6 ± 0.1 ka. This age of deglaciation is confirmed with ^{10}Be ages of 9.9 ± 0.1 ka from an island adjacent to the historical ice position. The lake sediment sequences also constrain the ice margin to have been less extensive than it is today for the remainder of the Holocene until ~1100 to ~700 yr ago, when it advanced into two lake catchments. The ice margin retreated back out of these lake catchments in the last decade. The early Holocene deglaciation in Melville Bugt, one of few locations around Greenland where a vast stretch of the current ice margin is marine-based, preceded deglaciation in most other parts of Greenland. Earlier deglaciation in this ice-sheet sector may have been caused by additional ablation mechanisms that apply to marine-based ice margins. Furthermore, despite ice-sheet models depicting this sector of Greenland as relatively stable throughout the Holocene, our data indicate a >20 km advance-retreat cycle within the last millennium.

© 2013 University of Washington. Published by Elsevier Inc. All rights reserved.

Introduction

Understanding the sensitivity of the Greenland Ice Sheet to ongoing and future climate change will narrow uncertainties about future sea-level rise (Alley et al., 2010). Yet, the observational record of ice-sheet behavior reveals a complex relationship to climate change (e.g., Kelley et al., 2012). Reconstructions of Greenland Ice Sheet changes during the Holocene provide a longer-term period over which to examine ice-sheet response to climate change. In addition, constraints on ice-margin positions spanning the Holocene provide tests for numerical ice-sheet models (e.g., Simpson et al., 2009). However, despite the emergence of new glacial chronologies from around Greenland, detailed reconstructions of ice-margin positions during the Holocene remain geographically sparse.

Northwestern Greenland consists largely of marine-based ice margins with fast-flowing outlet glaciers and ice streams entering Melville Bugt over and between dozens of island archipelagos, peninsulas, nunataks and seminunataks (Fig. 1). A major outlet glacier in northwestern Greenland is Upernavik Isstrøm, which comprises four distinct branches (Nielsen et al., 2012). The distance of retreat of Upernavik Isstrøm since the first historical observation in 1849 (~20–30 km) rivals that of other fast flowing outlet glaciers along western Greenland, such as Jakobshavn Isbræ (~40 km) and Kangiata Nunata Sermia (~20 km; Weidick, 1958, 1968; Weidick et al., 2012; Csatho et al., 2008).

The chronology of ice-margin retreat from the latest Pleistocene maximum position on the continental shelf (Funder et al., 2011; Ó Cofaigh et al., 2013) to the Holocene minimum behind the current ice margin was variable throughout Greenland (Bennike and Björck, 2002). For example, deglaciation occurred 9.6 to 9.1 ka at sites in northern Melville Bugt and >10 ka at some localities in southern Greenland, yet it occurred much later (as late as 6.2 ka) elsewhere around Greenland (Bennike and Björck, 2002). Little is known about the glacial history of Melville Bugt because few studies have focused on ice-margin changes there during the Holocene (Bennike, 2008; Funder et al., 2011).

Numerical ice-sheet models depict significant inland retreat of the western Greenland Ice Sheet during the middle Holocene (e.g., Simpson et al., 2009). In this area, there is also terrestrial evidence to support model depictions of the ice margin being inland of its present position during the early–middle Holocene (e.g., Weidick, 1968; Long et al., 2009). The margin of the ice sheet reestablished a position similar to the present location during the last few centuries—during the Little Ice Age (LIA; 1250–1900 AD; Kaplan et al., 2002; Weidick, 1968; Weidick and Bennike, 2007; Weidick et al., 2012; Briner et al., 2010). These same models depict a non-fluctuating, relatively stable ice-sheet position throughout the Holocene elsewhere around Greenland, including the Melville Bugt region. However, there are few field data available from Melville Bugt to compare with these modeling results.

Here, we use ^{10}Be dating and radiocarbon-dated sediment cores from proglacial-threshold lakes adjacent to Upernavik Isstrøm to constrain ice-margin positions throughout the Holocene. Our goal is to add information

* Corresponding author.
E-mail address: jbriner@buffalo.edu (J.P. Briner).
[1] Current address: Department of Geology, Lund University, Sölvegatan 12, S-22362 Lund, Sweden.

0033-5894/$ – see front matter © 2013 University of Washington. Published by Elsevier Inc. All rights reserved.
http://dx.doi.org/10.1016/j.yqres.2013.09.008

https://doi.org/10.1016/j.yqres.2013.09.008 Published online by Cambridge University Press

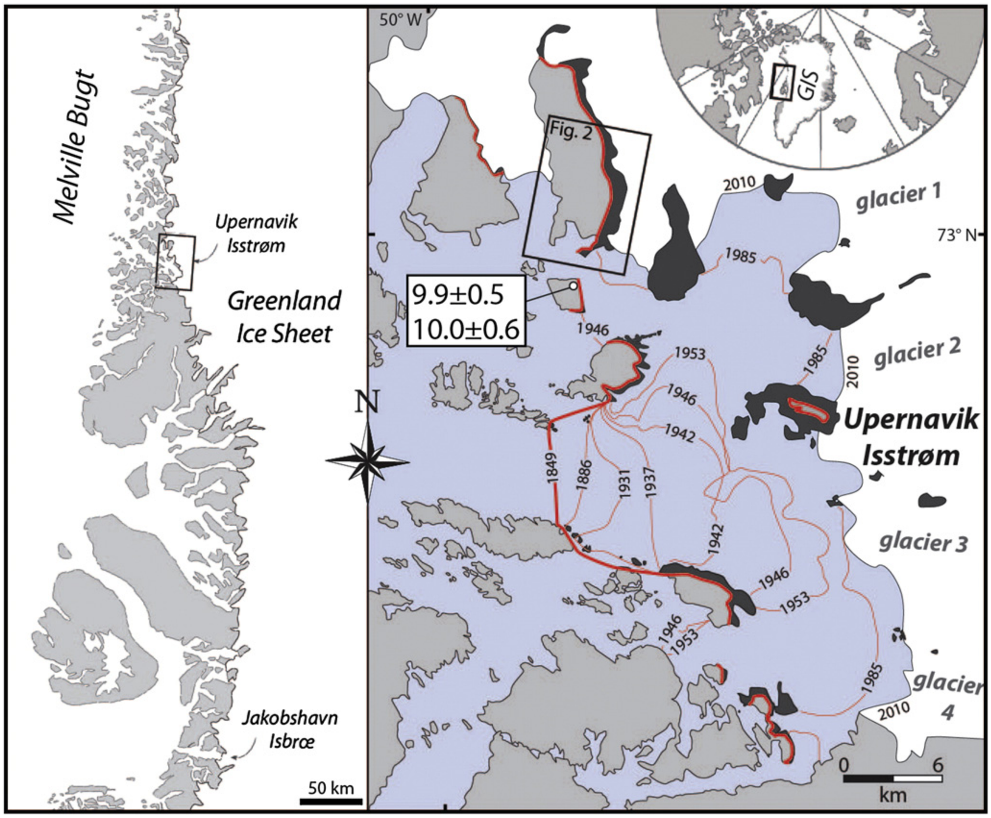

Figure 1. Map of western Greenland (location shown in inset map; GIS = Greenland Ice Sheet) showing the location of Melville Bugt and Upernavik Isstrøm. Ice limits in right panel from Weidick (1958), supplemented with 1985 aerial photographs; ice limit on base map from 2010 LANDSAT image. Bold red line marks the historical moraine, interpreted as the culmination of the Neoglacial advance of the Upernavik Isstrøm system; dark gray areas are recently deglaciated landscapes. Two ages in white box are ^{10}Be ages expressed in ka.

from a part of Greenland where few data exist to see how the glacial history here compares with elsewhere around Greenland. Given the spatial and temporal heterogeneity of contemporary ice-sheet changes, it is relevant to determine if the pattern of ice-margin changes throughout the Holocene exhibits variability as well. Specifically, we aim to: 1) constrain the timing of late Pleistocene–Holocene deglaciation at Upernavik Isstrøm, and 2) determine if the significant retreat of Upernavik Isstrøm in the past 160 yr followed a brief period of maximum extent during the LIA like at Jakobshavn Isbræ (Briner et al., 2011), or instead followed a more long-lived ice-margin position consistent with depictions from ice-sheet models.

Setting and methods

Upernavik Isstrøm terminates at the head of the iceberg-choked Upernavik Isfjord, ~70 km from Melville Bugt (Fig. 1). The bedrock is Precambrian charnockite (orthopyroxene-bearing granite; Escher, 1985), and the lakes are soft-water lakes. We collected sediment cores from three lakes near the Upernavik Isstrøm margin in 2011. No suitable lakes existed adjacent to the four individual branches that comprise Upernavik Isstrøm; our study lakes lie adjacent to an outlet glacier adjacent to the northernmost branch (Nielsen et al., 2012; Fig. 1). We targeted one non-glacial lake and two proglacial-threshold lakes that received meltwater from the ice sheet until the early 2000s AD according to satellite images that date back to 1972 (Fig. 2). The bathymetry of the three lakes was surveyed using a Garmin GPSMAP 400 series GPS receiver connected to a dual-beam echo sounder. Bathymetric maps were created by importing GPS-derived waypoints into the ArcGIS package where contours were generated automatically (note that contours away from bathymetric measurements are poorly constrained). Coring was executed using a Universal Coring system (www.aquaticresearch.com), which can collect cores up to 2 m in length with an intact sediment–water interface. In surface cores, the water above the sediments was drained iteratively using a small awl hole at the interface as the sediment cores were kept vertical for several days. Sediment cores were subsequently packed with floral foam and capped for transport and cold storage.

Primary Lake (all lake names are informal; 280 m asl) is the northernmost and largest of the three lakes cored (Fig. 2), and imagery reveals that it transitioned from a proglacial to non-glacial lake from AD 2003 to 2008. Primary Lake is located west of the historical moraine [Weidick (1968) termed the moraines that are generally regarded as having been deposited during the LIA the "historical moraines;" because these moraines, which represent the maximum late Holocene extent of the ice sheet, can post-date the LIA (Kelley et al., 2012), we refer to them herein as the historical moraine]. A ~1-km-long meltwater stream spans from the historical moraine to the northeastern corner of the lake. Secondary Lake (167 m asl) is the southernmost lake that we cored; imagery reveals that its transition from a proglacial to non-glacial state is ongoing, and was initiated sometime after 1985. The lake is only ~0.1 km west of the historical moraine and its southeastern shoreline is fronted by a proglacial delta that was the sediment source during proglacial conditions. Finally, Foster Lake (198 m asl), which is located between Primary and Secondary lakes, did not receive meltwater from the Greenland Ice Sheet margin during the late Holocene, and thus has been a non-glacial lake since deglaciation.

We report 15 radiocarbon ages from five sediment cores (Table 1). Macrofossil samples (n = 8) picked and cleaned with de-ionized water and bulk-sediment samples (n = 7) were submitted to the National Ocean Sciences Accelerator Mass Spectrometry Facility at

https://doi.org/10.1016/j.yqres.2013.09.008 Published online by Cambridge University Press

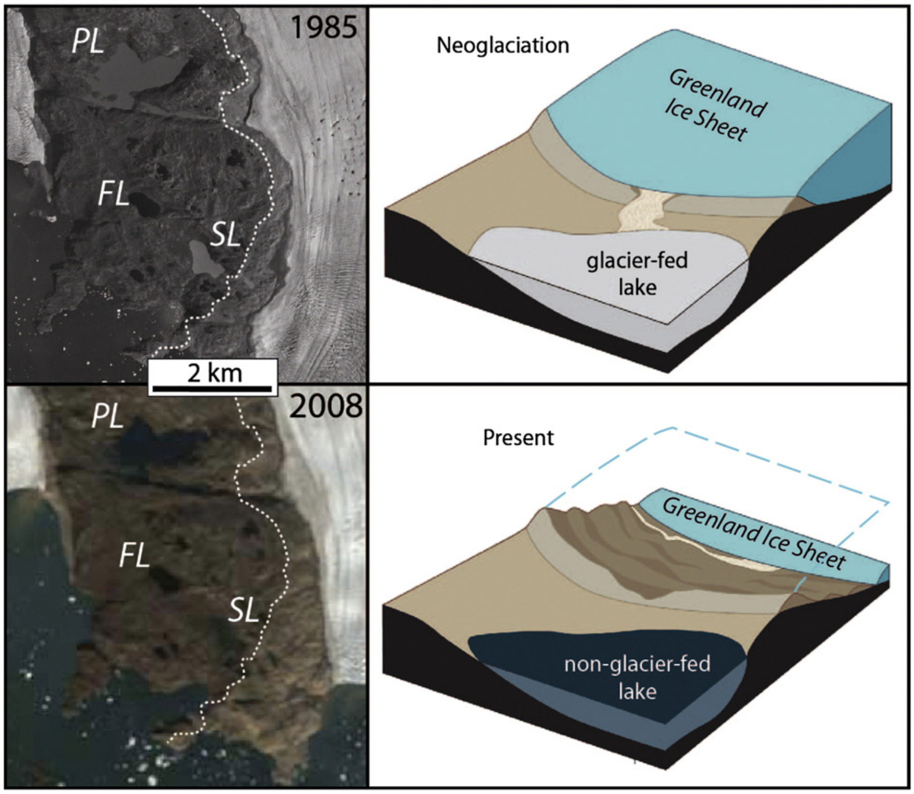

Figure 2. Primary (PL) and Secondary (SL) lakes shown in 1985 AD as meltwater-fed proglacial lakes (gray-colored surface indicates suspended sediment load) and in 2008 AD as low-turbidity, non-glacial-fed lakes. Both lakes fed from ice source on the right (east) side of the image. Historical moraine shown as dashed line. Imagery throughout this interval reveals that PL and SL became mostly clear during a ~5 yr interval between 2004 and 2008. 2010 images, although of poor quality (not shown), reveal that the two lakes are even clearer than depicted in the 2008 image. Cartoons at right show a "proglacial-threshold" lake in the proglacial state during Neoglaciation (top) and a non-glacial state (bottom). FL = Foster Lake. The location of the images is shown in Fig. 1.

Woods Hole Oceanographic Institution. We calibrated all ages using CALIB html version 6.0 with the INTCAL09 dataset (Stuiver et al., 2005) and report the mean age with two-standard deviation uncertainty, calculated by taking the midpoint of the two-standard deviation age range. Magnetic susceptibility (MS), a measure of the relative amount of minerogenic material in the sediment, was performed on all split cores at 0.5 cm contiguous intervals using a Bartington MS2E High Resolution Surface Scanning Sensor scanner connected to a Bartington MS2 Magnetic Susceptibility Meter. Percent loss-on-ignition (LOI) at 550°C, a measure of sediment organic matter content, was measured on an aliquot of freeze-dried sub-samples collected every 0.5 cm from 11PRM-1.

To bolster basal radiocarbon ages from our lake sites, two samples were collected for ^{10}Be dating from a small island (south of the lake

Table 1
Radiocarbon ages from lakes near Upernavik Isstrøm.

Core	Depth (cm)	Lab number	Material dated	δ^{13}C (‰PDB)	Radiocarbon age (^{14}C yr BP)	Calibrated age (cal yr BP)	Calibrated 2σ age range (cal yr BP)
Primary Lake (280 m asl)							
11PRM-1	3.0–3.8	OS-92902	*Salix* sp., *Polytrichum* sp.	−23.45	1370 ± 55	1280 ± 100	1178–1375
11PRM-1	5.0–5.3	OS-92468	Plant/wood	−23.39	625 ± 30	610 ± 50	552–660
11PRM-1	25.0–25.3	OS-92412	*Warnstorfia exannulata*	−23.93	2700 ± 25	2800 ± 50	2758–2849
11PRM-1	43.5–44.0	OS-92413	*Warnstorfia exannulata*	−26.20	4730 ± 35	5450 ± 130	5326–5583
11PRM-1	65.0–66.0	OS-92414	*Warnstorfia exannulata*	−26.02	6070 ± 35	7020 ± 130	6797–7146
11PRM-1	88.0–89.0	OS-92424	*Warnstorfia exannulata*	−23.25	7750 ± 35	8470 ± 40	8434–8594
11PRM-2	3.5–3.8	OS-96910	Sediment–organic carbon	−28.86	1110 ± 35	1030 ± 90	933–1122
11PRM-2	6.2–6.5	OS-97071	Sediment–organic carbon	−26.86	7450 ± 25	690 ± 30	664–724
11PRM-2	101.3–101.6	OS-92415	*Scorpidium scorpioides*	−25.10	8360 ± 40	9370 ± 90	9285–9474
Secondary Lake (167 m asl)							
11SND-3	24.5–24.8	OS-92441	Sediment–organic carbon	−28.61	1130 ± 25	1070 ± 100	963–1166
11SND-3	46.5–47.0	OS-92442	*Warnstorfia exannulata*	−31.82	8320 ± 45	9300 ± 160	9141–9466
11SND-3	46.5–47.0	OS-92443	Sediment–organic carbon	−29.98	8170 ± 35	9140 ± 120	9015–9255
11SND-3	62.0–62.3	OS-92444	Sediment–organic carbon	−27.97	4240 ± 30	4760 ± 100	4653–4859
11SND-2	40.0–40.3	OS-97072	Sediment–organic carbon	−28.65	1150 ± 30	1070 ± 100	977–1170
Foster Lake (198 m asl)							
11FST-2	56.7–57.0	OS-92445	Sediment–organic carbon	−27.73	8580 ± 35	9550 ± 50	9491–9599

Note: *Salix* sp., and *Polytrichum* sp. are terrestrial; *Warnstorfia exannulata* and *Scorpidium scorpoides* are aquatic.

https://doi.org/10.1016/j.yqres.2013.09.008 Published online by Cambridge University Press

sites) upon which the historical moraine is draped (Fig. 1). The island lies along the northern portion of Upernavik Isfjord, and its exposure age is expected to represent the time when Upernavik Isstrøm and the adjacent ice margin last deglaciated from this portion of the fjord. Samples 11GRO-7 (72° 58.725′ N; 54° 46.902′ W; 36 m asl) and 11GRO-8 (72° 58.438′ N; 54° 46.318′ W; 97 m asl) were collected from an erratic cobble resting directly on bedrock and a glacially polished quartz vein in bedrock, respectively, using a hammer and chisel (Fig. 5). Both samples are above the marine limit, which is thought to be 20 m or less in this part of Greenland based on raised marine features (or lack thereof; Fredskild, 1985; Funder and Hansen, 1996). We found no evidence in the field area of raised marine features above present sea level. In addition, like many landscapes around the Greenland Ice Sheet that were glaciated by fast-flowing glaciers, the landscape from which our samples are from is dominated by broad areas of clean, ice-sculpted bedrock draped with erratic cobbles and boulders. Thus, we think it is unlikely that either the cobble or bedrock sample was exhumed sometime following deglaciation. Sample sites have negligible topographic shielding, which was checked with a clinometer. We recorded geographic coordinates and elevation with a handheld GPS device with an estimated error of ±10 m.

Chemical processing of the two rock samples took place at the University of Buffalo Cosmogenic Nuclide Laboratory following standard Be isolation methods (Young et al., 2013). All $^{10}Be/^{9}Be$ ratios were measured at the Lawrence Livermore National Laboratory Center for Accelerator Mass Spectrometry relative to the 07KNSTD standard with a reported ratio of 2.85×10^{-12} (Nishiizumi et al., 2007; Rood et al., 2010) and corrected for a background procedural blank (Table 1). ^{10}Be ages were calculated using the CRONUS-Earth online calculator (http://hess.ess.washignton.edu/math; Version 2.2; Balco et al., 2008) applying a locally calibrated ^{10}Be production rate (Briner et al., 2012) and the Lal/Stone scaling scheme (Lal, 1991; Stone, 2000). Corrections for snow cover were not made because the sampled surfaces are from high points in the landscape and considered to be windswept of snow. Evidence of glacial abrasion on the bedrock surface indicates negligible post-glacial erosion.

Results

We collected two adjacent sediment cores from the deepest part of a small sub-basin in the northwestern corner of Primary Lake, near its outlet (Fig. 3). The sub-basin has a maximum depth of 7.3 m. The two sediment cores (73° 2.053′ N; 54° 47.296′ W), 11PRM-1 and 11PRM-2, have a similar stratigraphy of alternating organic-rich and mineral-rich sediments, bounded by sharp contacts typical of proglacial-threshold lakes (Kaplan et al., 2002; Briner et al., 2010). Both sediment cores contain mineral-rich sediment units at their surfaces. The upper 2–3 cm of both cores is mineral-rich, below which to a depth of ~5 cm is a mixture of mineral- and organic-rich sediment layers (Fig. 4). Below this upper unit of mostly mineral-rich sediments, the cores comprise a thick unit of organic-rich sediment. 11PRM-2 extends to 105 cm depth, the bottom 3 cm of which contains mineral-rich sediments; 11PRM-1 ends at 96 cm depth and did not retain mineral-rich sediments at its base.

We collected two sediment cores from Secondary Lake. 11SND-2 (73° 0.325′ N; 54° 43.734′ W) was collected from 16.8 m depth, in the deepest part of the single-basin lake, and 11SND-3 (73° 0.377′ N, 54° 43.820′ W) was collected from 12.5 m depth on the portion of the lake basin opposite the inflow delta (Fig. 3). 11SND-2 contains 39 cm of laminated mineral-rich sediment overlying organic-rich sediments to a depth of 86 cm; the bottom 3 cm of the core comprises mineral-rich sediments (Fig. 4). 11SND-3 contains 25 cm of laminated mineral-rich sediment overlying organic-rich sediment to a depth of 49 cm. Mineral-rich sediments span from 49 to 62 cm, below which a conspicuous unit of organic-rich sediment extends to the core base at 64 cm.

We also collected two cores from Foster Lake, which has a maximum depth of 19 m (Fig. 3). 11FST-1 (73° 0.889′ N; 54° 45.597′ W) was

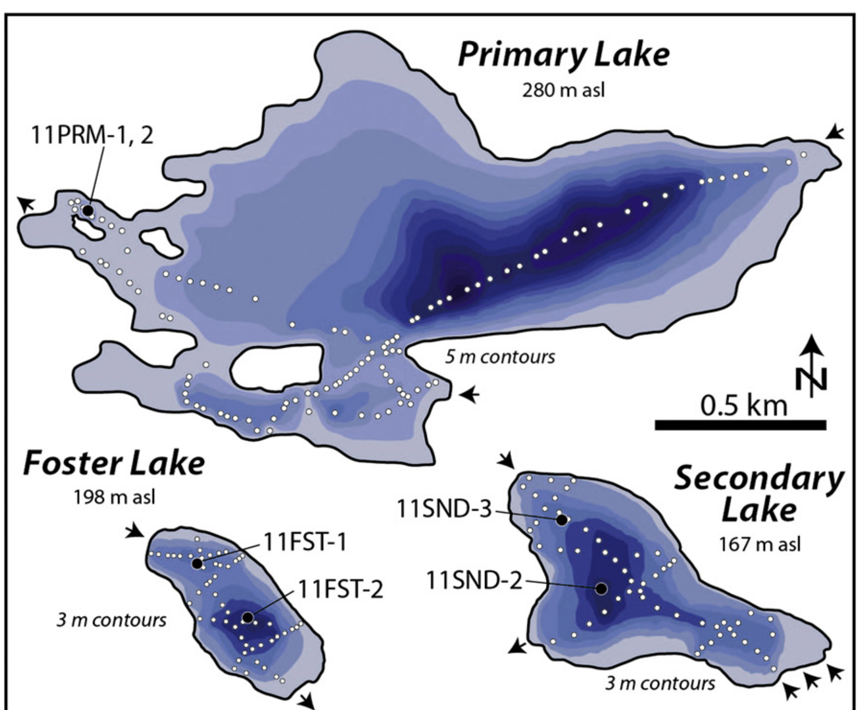

Figure 3. Bathymetry and core locations of the three study lakes. Contours are interpolated from locations with bathymetry data (white dots; see text). All lakes are shown at same scale; arrows show locations of inflows and outflows.

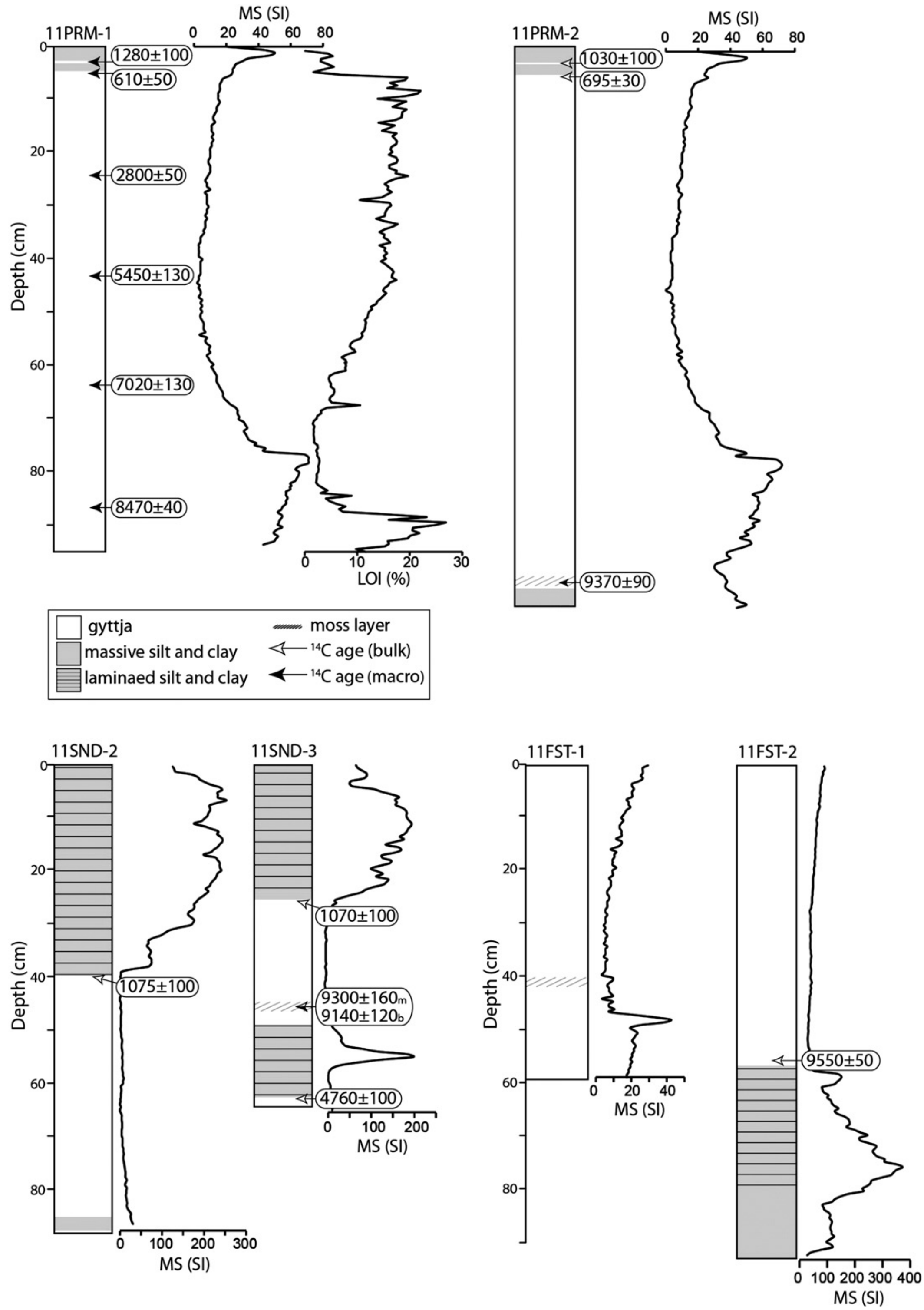

Figure 4. Lithostratigraphic logs of all sediment cores with radiocarbon ages in cal yr BP.

collected from 8.2 m depth, is 59 cm long, and contains organic-rich sediment throughout (Fig. 4). 11FST-2 (73° 0.810′ N; 54° 45.377′ W) was collected from 15.0 m depth, is 93 cm long, and contains 58 cm of organic-rich sediment overlying 35 cm of mineral-rich sediment.

The 15 radiocarbon ages range from 9550 ± 50 cal yr BP to 610 cal yr BP (Table 1; Fig. 4). Four radiocarbon ages are from organic-rich sediments nearest the contact with basal mineral-rich sediments. An age of 9370 ± 90 cal yr BP is from 11PRM-2 (macrofossil-based age) and an age of 9550 ± 50 cal yr BP is from 11FST-2 (bulk-sediment-based age). Two samples from the same depth in 11SND-3 are 9300 ±160 cal yr BP (macrofossil-based age) and 9140 ± 120 cal yr BP (bulk-sediment-based age).

Six radiocarbon ages from uppermost organic-rich sediments, nearest the contact with overlaying mineral-rich sediments, range from 1280 ± 100 cal yr BP to 610 ± 50 cal yr BP. These include two bulk-sediment ages from the Secondary Lake cores, which are 1075 ± 100 cal yr BP (11SND-2) and 1070 ± 100 cal yr BP (11SND-3). The uppermost sediments in both Primary Lake cores were also dated, and in

https://doi.org/10.1016/j.yqres.2013.09.008 Published online by Cambridge University Press

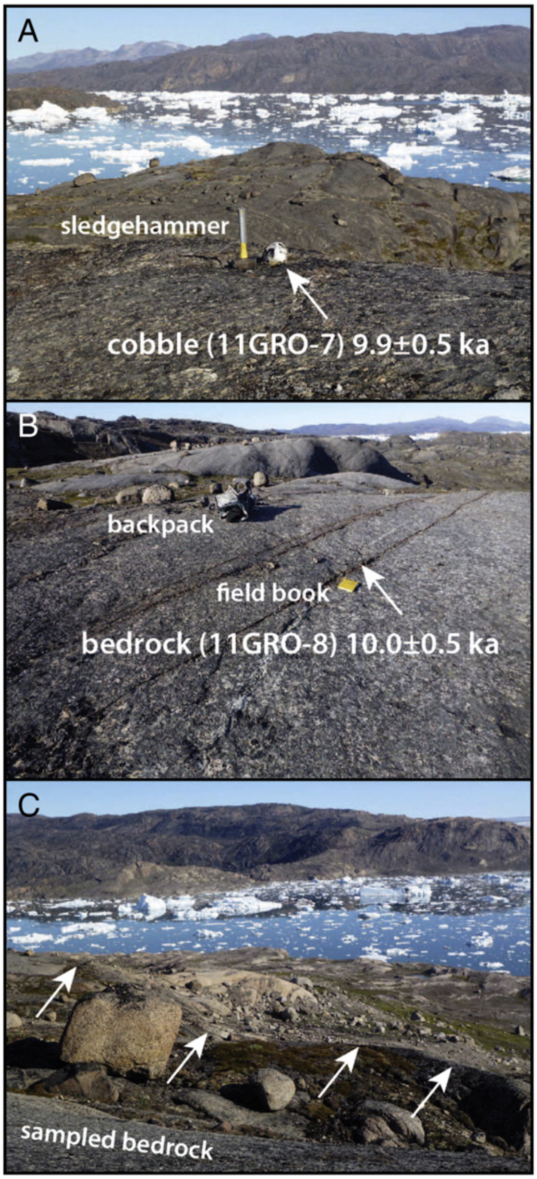

Figure 5. Photographs from a small island within Upernavik Isfjord where two samples for ^{10}Be dating were collected. A. Sample 11GRO-7, a quartz cobble resting on ice-sculpted bedrock; sledgehammer for scale. B. Sample 11GRO-8, a thin quartz vein from an ice-sculpted bedrock outcrop, field book and backpack for scale. C. View to the north; bedrock outcrop from which 11GRO-8 was collected is seen at the bottom of the photograph. Arrows point to the historical moraine and trimline. In the distance, beyond the island to the north is the peninsula where the study lakes reside.

both cases yield age reversals. In 11PRM-1, an age of terrestrial plant macrofossils from 3 cm is 1280 ± 100 cal yr BP, and an age of aquatic mosses from 5 cm is 610 ± 50 cal yr BP. Similarly, in 11PRM-2, a bulk-sediment-based age from 3.5 cm is 1030 ± 90 cal yr BP, and a bulk-sediment-based age from 6.2 cm is 690 ± 30 cal yr BP.

Four aquatic moss-based ages were obtained from organic-rich sediments throughout 11PRM-1. These four samples yield ages in stratigraphic order: 8470 ± 40 cal yr BP (88 cm), 7020 ± 130 cal yr BP (65 cm), 5450 ± 130 cal yr BP (43.5 cm) and 2800 ± 50 cal yr BP (25 cm). In addition, a single bulk-sediment-based age from the conspicuous, thin organic unit at the base of the 11SND-2 core yields an age of 4240 ± 30 cal yr BP. Finally, the two ^{10}Be ages are 9.9 ± 0.5 ka (erratic cobble) and 10.0 ± 0.6 ka (ice-polished quartz vein in bedrock; Table 2).

Interpretation

The lake-sediment stratigraphies and radiocarbon chronologies reveal a general pattern of Upernavik Isstrøm retreating in the early Holocene and remaining more restricted than its present position during the remainder of the Holocene until sometime during the last millennium, when it advanced into the Primary and Secondary lake catchments. Our most direct age control on the timing of deglaciation is from the pair of ^{10}Be ages, which average 9.9 ± 0.1 ka. Consistent with this age for the last deglaciation are the four basal radiocarbon ages that range from 9.1 to 9.6 cal yr BP that provide minimum-limiting ages for deglaciation. The radiocarbon ages are younger than the ^{10}Be ages; however, they are 0.25 to 1.5 cm above the contact between mineral-rich sediments and organic-rich sediments, and thus they provide minimum ages only. We do not know for how long the mineral-rich sediments were deposited in the lakes after deglaciation of the catchments and prior to the onset of organic-rich sedimentation. It is also possible that stagnant ice was present in the lake basins for some time following ice retreat from the lake catchments. The radiocarbon age from the basal organic-rich sediments in 11SND-3 of 4.8 ka is incompatible with the rest of our chronology; we suggest that while raising the core, the bottommost 2 cm of mineral-rich sediments slipped out and the void was filled with organic-rich sediments as the core was being raised through the sediment column.

The distribution of ages throughout the organic-rich sediments in 11PRM-1 suggests that the ice margin was no more extensive than its current (2008–2012) position until the latest Holocene. The single unit of organic-rich sediments in the Secondary Lake sediment sequences also supports this interpretation. The closely limiting maximum ages for the upper organic-to-minerogenic sediment contact in the SND cores of 1070 and 1075 cal yr BP, each from a core in different locations within the lake basin, suggest that the ice margin advanced into the Secondary Lake basin shortly after this time.

The age assignment for the ice-margin advance into the Primary Lake catchment during the late Holocene is complicated by the age-reversals in the PRM cores. The age reversals, replicated in both sediment cores and with both macrofossil- and bulk-sediment-based ages, are difficult to explain. It is hard to envision a plausible way in which a radiocarbon age from both macrofossils and bulk sediments can be younger than their corresponding stratigraphic level. On the other hand, there are more geologically reasonable processes that can lead to a radiocarbon age that is too old for its stratigraphic level. One process could be mass movement of previously deposited organic matter from elsewhere in the basin to the core sites. Given the small and steep-sided sub-basin in which the adjacent cores were retrieved, we wonder if there was some slumping once the lake bottom began to be loaded with relatively

Table 2
^{10}Be ages of rock samples collected near Upernavik Isstrøm.

Sample	Latitude	Longitude	Elevation (m asl)	Sample type	Thickness (cm)	Shielding correction	Quartz (g)	^{9}Be carrier (μg)	^{10}Be ± 1σ (10^4 atoms g^{-1})	^{10}Be age (ka)
11GRO-7	72° 58.721′ N	54° 47.039′ W	36	Cobble on bedrock	3	1	50.0372	262	4.25 ± 0.11	9.85 ± 0.54
11GRO-8	72° 58.424′ N	54° 46.455′ W	97	Bedrock surface	1	1	30.0178	262	4.69 ± 0.12	10.00 ± 0.55

Note: Blank-corrected ratios are reported relative to the 07KNSTD standard (2.85 × 10^{-12}; Nishiizumi et al., 2007). Process blank for this sample batch is 9.627e − 16. We used 0.65 g of 405.2 ppm Be carrier.

https://doi.org/10.1016/j.yqres.2013.09.008 Published online by Cambridge University Press

dense mineral-rich sediment after the lake's transition from non-glacial to proglacial. Alternatively, bioturbation could give rise to such an age reversal, in which case the younger ages would be anomalous. However, if the minerogenic sediments were deposited after ~1000 yr AD, then there would be no organic-rich lacustrine sediment at a higher level from which to mix into lower layers. In addition, there is no visual evidence for bioturbation. Thus, we favor the slumping hypothesis, in which case the two radiocarbon ages of 610 and 690 cal yr BP are the more accurate maximum-limiting ages for the advance of the ice margin into the Primary Lake catchment.

We dated both macrofossils and bulk sediments, and in many cases our ages can be used to assess their relative suitability for dating lake sediments. Elsewhere in western Greenland, previous work has found that bulk sediments can yield radiocarbon ages a few hundred years older than macrofossils from the same levels (Kaplan et al., 2002; McGowan et al., 2003; Bennike et al., 2010). However, we find little evidence that bulk sediments in these lakes yield older radiocarbon ages than macrofossils in the same levels. For example, the pair of bulk-sediment- and aquatic-moss-based ages from 11SND-3 overlap at one sigma. Furthermore, the radiocarbon ages from the same stratigraphic positions in the two PRM cores – one set from aquatic mosses and one set from bulk sediments – yield ages that overlap at two sigma. We suggest that ultimately, the utility of dating bulk sediments should be evaluated on a lake-by-lake basis. However, once confirmed to yield ages comparable to macrofossil-based ages, bulk sediments can yield reliable radiocarbon chronologies in soft-water lakes in western Greenland.

Discussion

To place our age of deglaciation into context, we compiled the closest ages (^{14}C and ^{10}Be) to the historical ice limit around the Greenland Ice Sheet (Fig. 6). The compilation reveals that the spatio-temporal pattern of deglaciation varies around Greenland (Bennike and Björck, 2002; Bennike, 2008). In particular, the time when the ice-sheet margin retreated to, or inland of, its present position occurred earlier in Melville Bugt than most locations elsewhere around Greenland (Funder and Hansen, 1996; Bennike and Björck, 2002). Previous minimum age constraints on the retreat of ice in central Melville Bugt are provided by radiocarbon-dated basal lake sediments of 9.6 $\pm$ 0.3 ka (Fredskild, 1985) and a whale bone that was reworked into a historical moraine dated to 9.1 $\pm$ 0.1 ka (Bennike, 2008). Our ^{10}Be age assignment of 9.9 $\pm$ 0.1 ka and oldest minimum radiocarbon age of 9.6 $\pm$ 0.1 ka are consistent with these previous findings, and together confirm the relatively early deglaciation for the Melville Bugt sector of the Greenland Ice Sheet.

The other sector of the Greenland Ice Sheet that deglaciated relatively early is along the southern and southeastern coasts (Fig. 6). Sites along the Qassimiut lobe in southern Greenland became deglaciated shortly before ~9 ka (Weidick et al., 2004). There is a lack of deglaciation ages available from the southeastern coastline, but one recent study revealed that the landscape fronting Helheimgletscher deglaciated ~10.8 ka (Hughes et al., 2012). In contrast, deglaciation ages from other parts of Greenland show that the margin of the Inland Ice attained a position similar to the present – or inland of it – considerably later, ranging from 7 to 8 ka in parts of southwestern and northeastern Greenland, and even later, ~6–7 ka, in northern Greenland (Fig. 6; Bennike, 2008; Funder et al., 2011).

Unlike some sectors of the Greenland Ice Sheet that experienced terrestrial-based deglaciation, the Melville Bugt region encompassed deglaciation in largely marine-based environments. In many locations, the ice margin resides in deep marine troughs, many of which extend at least 50 km behind the present ice margin (Griggs et al., 2012). It has been previously hypothesized that ice retreated relatively early in the Melville Bugt sector because it was susceptible to rapid retreat via calving (e.g., Bennike, 2008). In addition, not only would the marine-

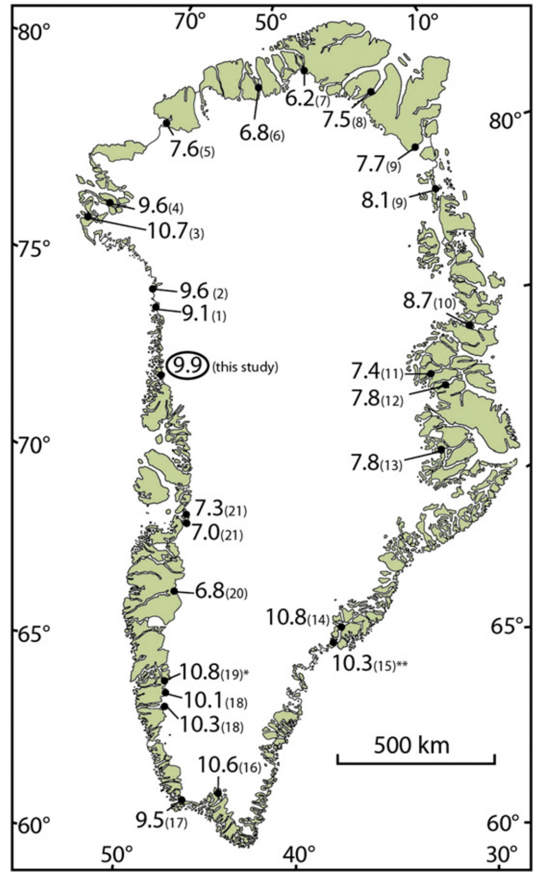

Figure 6. Map of Greenland showing the distribution of the closest ages (^{14}C and ^{10}Be) to the historical ice limit around the Greenland Ice Sheet. Ages are presented in ka; see original reference for age uncertainty and other details. 1: Bennike (2008); 2: Fredskild (1985); 3, 4, 11: Weidick (1978); 5: Bennike (2002); 6: Kelly and Bennike (1992); 7: Landvik et al. (2001); 8: Funder (1982); 9: Bennike and Weidick (2001); 10: Weidick (1977); 12: Håkansson (1976); 13: Funder (1978); 14: Hughes et al. (2012); 15: Roberts et al. (2008); ^{10}Be ages adjusted for production rate to be consistent with more recent studies (14, 18, 20, 21); 16: Larsen et al. (2011); 17: Kaplan et al. (2002); 18: Larsen et al. (2013); 19: Weidick et al. (2012); the 10.8 ka age is from a bivalve that was reworked into a moraine assigned to 8.3–8.1 ka, and is interpreted as indicating initial deglaciation prior to a re-advance); 20: Levy et al. (2012); 21: Young et al. (2013).

based ice have ablated via calving, but it would also have been exposed to submarine melting, thought to be a confounding influence on the mass balance of marine-based ice sheets (e.g., Holland et al., 2008; Jenkins et al., 2010; Rignot et al., 2010). These processes of ablation would also have operated along the tidewater-dominated southeastern coastline, and thus perhaps it is not surprising that this is another location on Greenland with relatively early deglaciation.

We note that the pattern of landscape age immediately outboard of historical moraines around Greenland could also be influenced by the magnitude of (1) inland retreat during the middle Holocene, and (2) the late Holocene advance. To explain this further, consider Jakobshavn Isbræ, where the historical moraine abuts a landscape deglaciated 7.4 ka, beyond which lies the Fjord Stade moraines (deposited at 9.3 and 8.2 ka; Weidick and Bennike, 2007; Young et al., 2011a). Beyond the Fjord Stade moraines, the landscape was deglaciated ~10.2 ka. If Jakobshavn Isbræ had a more extensive advance during Neoglaciation, such that it overran the Fjord Stade moraines, then its historical position would reside adjacent to a landscape that deglaciated at 10.2 ka. Perhaps the reason that Jakobshavn Isbræ did not advance this far is because it retreated far inland during the middle Holocene. At Upernavik Isstrøm, on the other hand, it is possible that the ice margin did not retreat far inland during the middle Holocene, as is depicted by models, and thus even a relatively small Neoglacial advance could reach landscapes deglaciated at 9.9 ka, which could be analogous to landscapes beyond the Fjord Stade moraines at Jakobshavn Isbræ. Thus, the pattern of landscape age abutting historical moraines around Greenland could be due to a combination of the pace of deglaciation, the magnitude of inland retreat during middle Holocene warmth, and the magnitude of the Neoglacial advance.

Our radiocarbon chronology also allows us to constrain the maximum late Holocene advance of the Upernavik ice margin and to place its current retreat into a pre-historic context. Neoglaciation on Greenland was likely underway by 3–4 ka following peak thermal conditions in the middle Holocene (Dahl-Jensen et al., 1998; Bennike and Weidick 2001; Long et al., 2009; Young et al., 2011b; Funder et al., 2011). Along western Greenland, the ice advance to the position of the historic moraine generally occurred during the LIA (Kaplan et al. 2002; Weidick et al., 2004, 2012; Weidick and Bennike, 2007; Briner et al., 2010, 2011; Larsen et al., 2011; Young et al., 2011b). However, there are some exceptions to this. In some cases the culmination of the Neoglacial advance has been found to post-date the LIA entirely (Weidick, 2009; Kelley et al., 2012), and in at least one case, it pre-dates the LIA significantly (e.g., Bennike and Sparrenbom, 2007). Our maximum-limiting ages from Secondary Lake of ~1070 cal yr BP leave open the possibility that ice entered this catchment a few hundred years prior to the LIA. On the other hand, our favored interpretation of the ages from Primary Lake is that ice advanced into that catchment after ~600 cal yr BP. Although ice retreated from both catchments around the same time, it is plausible that ice entered the catchments at different times, because the lakes and the drainage divides of their catchments are located at different elevations. Thus, interpreting our chronology conservatively, the Upernavik ice margin advanced to near its maximum latest Holocene position between ~1000 and 600 cal yr BP. Based on the observation that Upernavik Isstrøm was residing at or very near its historical moraine by Rink in 1849 AD (Weidick, 1958), we suggest that the culmination of the Neoglacial advance occurred during the late LIA period, similar to Jakobshavn Isbræ (Briner et al., 2011). Furthermore, if the Upernavik Isstrøm terminus is positioned today as it was prior to 1849 AD (~20 km down flowline from our study area), as inferred from our constraints of the ice margin position near our study lakes, then this implies that a ~20 km advance and retreat cycle took place within the LIA.

Unlike other records derived from proglacial-threshold lakes fringing the Greenland Ice Sheet margin (Kaplan et al., 2002; Briner et al., 2010, 2011; Larsen et al., 2011), which are either still proglacial or became ice-free sometime during the 20th century, the lakes studied here are unique in that they became ice-free in the past decade. This provides us with an opportunity to assess the precedence of the present position of the ice-sheet margin, especially following the dramatic retreat in recent years (Fig. 1; Weidick, 1958; Nielsen et al., 2012). For example, there are a number of recent studies demonstrating that Arctic glaciers have now receded, and Arctic climate has now warmed, to levels not seen since the middle Holocene (e.g., England et al., 2008; Fisher et al., 2012). In western Greenland, Jakobshavn Isbræ has receded so far that it is now situated in some places near its middle Holocene position as reconstructed by Weidick et al. (1990). Furthermore, at many locations around the Northern Hemisphere, alpine glaciers were at or very near their LIA positions during multiple glacier culminations throughout the entire Neoglacial interval (Clague et al., 2009; Briner et al., 2009; Schimmelpfennig et al., 2012; Maurer et al., 2012; Badding et al., 2013). However, despite the lake basins adjacent to Upernavik Isstrøm becoming deglaciated so recently, they still only record the latest Neoglacial advance of this sector of the Greenland ice margin. Thus, given that the ice margin has retreated out of the lake catchments in the past decade, the Upernavik sector has most likely yet to retreat to its middle Holocene position.

Conclusions

Upernavik Isstrøm, a major ice stream that drains a substantial component of the northwestern Greenland Ice Sheet, has retreated significantly over the last 160 yr. We constrain the fluctuations of the broader Upernavik ice margin during the Holocene and compare its history with ice-margin sectors elsewhere around Greenland. Areas adjacent to the ice margin near Upernavik Isstrøm deglaciated around 10 ka, which is earlier than most other sectors of the Greenland Ice Sheet. We suggest that this is most likely due to the additional mechanisms of ablation that operate in marine-based ice sheet sectors versus land-based counterparts. A contributing factor may be the proximity of the ice-sheet margin with the open sea. Calving in deep embayments, combined with submarine melting from warm ocean currents that entered Baffin Bay in the early Holocene (e.g., Knudsen et al., 2008), is inferred as the causal mechanisms behind the observed pattern and timing of retreat. This model for retreat applies to other marine-based glaciers (Pfeffer, 2007; Briner et al., 2009), and seems to have been the case for southeastern Greenland also.

Upernavik Isstrøm has now retreated to a position that has not been occupied in the last 1100–700 yr. The advance of Upernavik Isstrøm into our study lake catchments was seemingly part of an ice-sheet-wide advance that was likely initiated in the middle Holocene and that culminated in most locations late during the LIA. Unlike some ice retreat in the Arctic that has now reached a position last maintained in the middle Holocene, this does not seem to be the case yet for the northwestern Greenland Ice Sheet margin. Almost certainly, the advance of the ice sheet during the last millennium is superimposed on a prolonged advance throughout the Neoglaciation. Despite differing responses to middle Holocene warmth depicted in models for the ice margin along western Greenland (Simpson et al., 2009), the synchronous culmination of major western Greenland ice streams late during the LIA implies that fast-flowing outlets respond similarly to centennial-scale climate change. Ultimately, more records like these will help to explain the complex ice-marginal dynamics documented in geological and historical archives, and ultimately reduce uncertainties about the future of the Greenland Ice Sheet and sea-level rise.

Acknowledgments

We thank Stefan Truex and Nicolás Young for quartz preparation for ^{10}Be analysis, Susan Zimmerman and Robert Finkel at Lawrence Livermore National Laboratory for Be measurements, Jens O. Svendsen in Upernavik for logistical support and the National Geographic Society for financial support.

References

Alley, R., Andrews, J., Brigham-Grette, J., Clarke, G., Cuffey, K., Fitzpatrick, J., Funder, S., Marshall, S., Miller, G., Mitrovica, J., 2010. History of the Greenland ice sheet: paleoclimatic insights. Quaternary Science Reviews 29, 1728–1756.

Badding, M.E., Briner, J.P., Kaufman, D.S., 2013. ^{10}Be ages of late Pleistocene deglaciation and Neoglaciation in the north-central Brooks Range, Arctic Alaska. Journal of Quaternary Science 28, 95–102.

Balco, G., Stone, J.O., Lifton, N.A., Dunai, T.J., 2008. A complete and easily accessible means of calculating surface exposure ages or erosion rates from ^{10}Be and ^{26}Al measurements. Quaternary Geochronology 3, 174–195.

Bennike, O., 2002. Late Quaternary history of Washington land, North Greenland. Boreas 31, 260–272.

Bennike, O., 2008. An early Holocene Greenland whale from Melville Bugt, Greenland. Quaternary Research 69, 72–76.

Bennike, O., Björck, S., 2002. Chronology of the last recession of the Greenland ice sheet. Journal of Quaternary Science 17, 211–219.

Bennike, O., Sparrenbom, C.J., 2007. Dating of the Narssarssuaq stade in southern Greenland. The Holocene 17, 279–282.

Bennike, O., Weidick, A., 2001. Late Quaternary history around Nioghalvfjerdsfjorden and Jøkelbugten, North-East Greenland. Boreas 30, 205–227.

Bennike, O., Anderson, N.J., McGowan, S., 2010. Holocene palaeoecology of south-west Greenland inferred from macrofossils in sediments of an oligosaline lake. Journal of Paleolimnology 43, 787–798.

Briner, J.P., Bini, A.C., Anderson, R.S., 2009. Rapid early Holocene retreat of a Laurentide outlet glacier through an Arctic fjord. Nature Geoscience 2, 496–499.

https://doi.org/10.1016/j.yqres.2013.09.008 Published online by Cambridge University Press

Briner, J.P., Stewart, H.A.M., Young, N.E., Phillips, W., Losee, S., 2010. Using proglacial-threshold lakes to constrain fluctuations of the Jakobshavn Isbræ ice margin, western Greenland, during the Holocene. Quaternary Science Reviews 29, 3861–3874.
Briner, J.P., Young, N.E., Thomas, E.K., Stewart, H.A.M., Losee, S., Truex, S., 2011. Varve and radiocarbon dating support the rapid advance of Jakobshavn Isbræ during the Little Ice Age. Quaternary Science Reviews 30, 2476–2486.
Briner, J.P., Young, N.E., Goehring, B.M., Schaefer, J.M., 2012. Constraining Holocene ^{10}Be production rates in Greenland. Journal of Quaternary Science 27, 2–6.
Clague, J.J., Menounos, B., Osborn, G., Luckman, B.H., Koch, J., 2009. Nomenclature and resolution in Holocene glacial chronologies. Quaternary Science Reviews 28, 2231–2238.
Csatho, B., Schenk, T., van der Veen, C.J., Krabill, W.B., 2008. Intermittent thinning of Jakobshavn Isbræ, West Greenland, since the Little Ice Age. Journal of Glaciology 54, 131–144.
Dahl-Jensen, D., Mosegaard, K., Gundestrup, N., Clow, G.D., Johnsen, S.J., Hansen, A.W., Balling, N., 1998. Past temperatures directly from the Greenland Ice Sheet. Science 282, 268–271.
England, J.H., Lakeman, T.R., Lemmen, D.S., Bednarski, J.M., Stewart, T.G., Evans, D.J.A., 2008. A millennial-scale record of Arctic Ocean sea ice variability and the demise of the Ellesmere Island ice shelves. Geophysical Research Letters 35, L19502.
Escher, J.C. 1985. Geological map of Greenland 1:5,000,000, Upernavik Isfjord. Copenhagen: Geological Survey of Greenland.
Fisher, D., Zheng, J., Burgess, D., Zdanowicz, C., Kinnard, C., Sharp, M., Bourgeois, J., 2012. Recent melt rates of Canadian arctic ice caps are the highest in four millennia. Global and Planetary Change 84–85, 3–7.
Fredskild, B., 1985. The Holocene vegetational development of Tugtuligssuaq and Qeqertat, Northwest Greenland. Meddelelser om Grønland. Geoscience 14 (20 pp.).
Funder, S., 1978. Holocene stratigraphy and vegetation history in the Scoresby Sund area, East Greenland. Bulletin. Grønlands Geologiske Undersøgelse 129, 66.
Funder, S., 1982. ^{14}C-dating of samples collected during the 1979 expedition to North Greenland. Rapport Grønlands Geologiske Undersøgelse 110, 9–14.
Funder, S., Hansen, L., 1996. The Greenland Ice Sheet: a model for its culmination and decay during and after the Last Glacial Maximum. Bulletin of the Geological Society of Denmark 42, 137–152.
Funder, S., Kjeldsen, K.K., Kjær, K.H., Ó Cofaigh, C., 2011. The Greenland Ice Sheet during the past 300,000 years: a review. In: Ehlers, J., Gibbard, P.L. (Eds.), Quaternary Glaciations: Extent and Chronology, Developments in Quaternary Science 2. Elsevier, Amsterdam, pp. 699–713.
Griggs, J.A., Bamber, J.L., Hurkmans, R.T.W.L., Dowdeswell, J.A., Gogineni, S.P., Howat, I., Mouginot, J., Paden, J., Palmer, S., Rignot, E., Steinhage, D., 2012. A new bed elevation dataset for Greenland. The Cryosphere Discussions 6, 4829–4860.
Håkansson, S., 1976. University of Lund radiocarbon dates IX. Radiocarbon 18, 290–320.
Holland, D.M., Thomas, R.H., de Young, B., Ribergaard, M.H., Lyberth, B., 2008. Acceleration of Jakobshavn Isbræ triggered by warm subsurface ocean waters. Nature Geoscience 1, 659–664.
Hughes, A.L.C., Rainsley, E., Murray, T., Fogwill, C.J., Schnabel, C., Xu, S., 2012. Rapid response of Helheim Glacier, southeast Greenland, to early Holocene climate warming. Geology 40, 427–430.
Jenkins, A., Dutriux, P., Jacobs, S.S., McPhail, S.D., Perrett, J.R., Webb, A.T., White, D., 2010. Observations beneath Pine Island Glacier in West Antarctica and implications for its retreat. Nature Geoscience 3, 468–472.
Kaplan, M.R., Wolfe, A.P., Miller, G.H., 2002. Holocene environmental variability in southern Greenland inferred from lake sediments. Quaternary Research 58, 149–159.
Kelley, S.E., Briner, J.P., Young, N.E., Babonis, G.S., Csatho, B., 2012. Maximum late Holocene extent of the western Greenland Ice Sheet during the late 20th century. Quaternary Science Reviews 56, 89–98.
Kelly, M., Bennike, O., 1992. Quaternary geology of western and central north Greenland. Rapport Grønlands Geologiske Undersøgelse 153 (34 pp.).
Knudsen, K.L., Stabell, B., Seidenkrantz, M.-S., Eiríksson, J., Blake Jr., W., 2008. Deglacial and Holocene conditions in northernmost Baffin Bay: sediments, foraminifera, diatoms and stable isotopes. Boreas 37, 346–376.
Lal, D., 1991. Cosmic ray labeling of erosion surfaces: *in situ* nuclide production rates and erosion models. Earth and Planetary Science Letters 104, 424–439.
Landvik, J.Y., Weidick, A., Hansen, A., 2001. The glacial history of the Hans Tausen Iskappe and the last glaciation of Peary Land. North Greenland. Meddelelser om Grønland. Geoscience 39, 27–44.
Larsen, N.K., Kjær, K.H., Olsen, J., Funder, S., Kjeldsen, K.K., Nørgaard-Pedersen, N., 2011. Restricted impact of Holocene climate variations on the southern Greenland Ice Sheet. Quaternary Science Reviews 30, 3171–3180.
Larsen, N.K., Funder, S., Kjær, K.H., Kjeldsen, K.K., Knudsen, M.F., Linge, H., 2013. Rapid early Holocene ice retreat in West Greenland. Quaternary Science Reviews (in press).
Levy, L.B., Kelly, M.A., Howley, J.A., Virginia, R.A., 2012. Age of Ørkendalen moraines, Kangerlussuaq, Greenland: constraints on the extent of the southwestern margin of the Greenland Ice Sheet during the Holocene. Quaternary Science Reviews 52, 1–5.
Long, A.J., Woodroffe, S.A., Dawson, S., Roberts, D.H., Bryant, C.L., 2009. Late Holocene relative sea level rise and the Neoglacial history of the Greenland Ice Sheet. Journal of Quaternary Science 24, 345–359.
Maurer, M.K., Menounos, B., Lucman, B.H., Osborn, G., Clague, J.J., Beedle, M.J., Smith, R., Atkinson, N., 2012. Late Holocene glacier expansion in the Cariboo and northern Rocky Mountains, British Columbia, Canada. Quaternary Science Reviews 51, 71–80.
McGowan, S., Ryves, D.B., Anderson, N.J., 2003. Holocene records of effective precipitation in West Greenland. The Holocene 13, 239–249.
Nielsen, K., Khan, S.A., Korsgaard, N.J., Kjær, K.H., Wahr, J., Bevis, M., Sterns, L.A., Timm, L.H., 2012. Crustal uplift due to ice mass variability on Upernavik Isstrøm, west Greenland. Earth and Planetary Science Letters 353–354, 182–189.
Nishiizumi, K., Imamura, M., Caffee, M., Southon, J., Finkel, R., McAninch, J., 2007. Absolute calibration of ^{10}Be AMS standards. Nuclear Instruments and Methods in Physics Research Section B: Beam Interactions with Materials and Atoms 258, 403–413.
Ó Cofaigh, C., Dowdeswell, J.A., Jennings, A.E., Hogan, K.A., Kilfeather, A., Hiemstra, J.F., Noormets, R., Evans, J., McCarthy, D.J., Andrews, J.T., Lloyd, J.M., Moros, M., 2013. An extensive and dynamic ice sheet on the West Greenland shelf during the last glacial cycle. Geology 41, 219–222.
Pfeffer, W.T., 2007. A simple mechanism for irreversible tidewater glacier retreat. Journal of Geophysical Research 112, F03S25.
Rignot, E., Koppes, M., Velicogna, I., 2010. Rapid submarine melting of the calving faces of west Greenland glaciers. Nature Geoscience 3, 187–191.
Roberts, D.H., Long, A.J., Schnabel, C., Freeman, S., Simpson, M.J.R., 2008. The deglacial history of southeast sector of the Greenland Ice Sheet during the Last Glacial Maximum. Quaternary Science Reviews 27, 1505–1516.
Rood, D.H., Hall, S., Guilderson, T.P., Finkel, R.C., Brown, T.A., 2010. Challenges and opportunities in high precision Be-10 measurements at CAMS. Nuclear Instruments and Methods in Physics Research Section B: Beam Interactions with Materials and Atoms 268, 730–732.
Schimmelpfennig, I., Schaefer, J.M., Akçar, N., Ivy-Ochs, S., Finkel, R.C., Schlüchter, C., 2012. Holocene glacier culminations in the western Alps and their hemispheric relevance. Geology 40, 891–894.
Simpson, M.J.R., Milne, G.A., Huybrechts, P., Long, A.J., 2009. Calibrating a glaciological model of the Greenland ice sheet from the last glacial maximum to present-day using field observations of relative sea level and ice extent. Quaternary Science Reviews 28, 1631–1657.
Stone, J.O., 2000. Air pressure and cosmogenic isotope production. Journal of Geophysical Research 105, 23,753–23,759.
Stuiver, M., Reimer, P.J., Reimer, R.W., 2005. CALIB 5.0. http://calib.qub.ac.uk/calib/.
Weidick, A., 1958. Frontal variations at Upernaviks Isstrøm in the last 100 years. Meddelelser fra Dansk Geologisk Forening 14, 52–60.
Weidick, A., 1968. Observations on some Holocene glacier fluctuations in West Greenland. Meddelelser om Grønland 165, 202.
Weidick, A., 1977. ^{14}C dating of survey material carried out in 1976. Rapport Grønlands Geologiske Undersøgelse 85, 127–129.
Weidick, A., 1978. ^{14}C dating of survey material carried out in 1977. Rapport Grønlands Geologiske Undersøgelse 90, 119–124.
Weidick, A., 2009. Johan Dahl Land, south Greenland: the end of a 20th century glacier expansion. Polar Record 45, 337–350.
Weidick, A., Bennike, O., 2007. Quaternary glaciation history and glaciology of Jakobshavn Isbrae and the Disko Bugt region, West Greenland: a review. Geological Survey of Denmark and Greenland Bulletin 14, 78.
Weidick, A., Oerter, H., Reeh, N., Thomsen, H.H., Thorning, L., 1990. The recession of the Inland Ice margin during the Holocene climatic optimum in the Jakobshavn Isfjord area of West Greenland. Palaeogeography, Palaeoclimatology, Palaeoecology 82, 389–399.
Weidick, A., Kelly, M., Bennike, O., 2004. Late Quaternary development of the southern sector of the Greenland Ice Sheet, with particular reference to the Qassimiut lobe. Boreas 33, 284–299.
Weidick, A., Bennike, O., Citterio, M., Nørgaard-Pedersen, N., 2012. Neoglacial and historical glacier changes around Kangersuneq fjord in southern West Greenland. Geological Survey of Denmark and Greenland Bulletin 27, 68.
Young, N.E., Briner, J.P., Axford, Y., Csatho, B., Babonis, G.S., Rood, D.H., Finkel, R.C., 2011a. Response of a marine-terminating Greenland outlet glacier to abrupt cooling 8200 and 9300 years ago. Geophysical Research Letters 38, L24701.
Young, N.E., Briner, J.P., Stewart, H.A.M., Axford, Y., Csatho, B., Rood, D.H., Finkel, R.C., 2011b. Response of Jakobshavn Isbræ Greenland, to Holocene climate change. Geology 39, 131–134.
Young, N.E., Briner, J.P., Rood, D.H., Finkel, R.C., Corbett, L.B., Bierman, P.R., 2013. Age of the Fjord Stade moraines in the Disko Bugt region, western Greenland, and the 9.3 and 8.2 ka cooling events. Quaternary Science Reviews 60, 76–90.

https://doi.org/10.1016/j.yqres.2013.09.008 Published online by Cambridge University Press